Crossover from the Quantum Critical to Overdamped Regime in the Heavy-Fermion System USn_3

S. Kambe,[1] H. Sakai,[1] Y. Tokunaga,[1] T. D. Matsuda,[1] Y. Haga,[1] H. Chudo,[1] and R. E. Walstedt[2]

[1]*Advanced Science Research Center, Japan Atomic Energy Agency, Tokai-mura, Ibaraki 319-1195, Japan*
[2]*Physics Department, The University of Michigan, Ann Arbor, Michigan 48109, USA*
(Received 24 October 2008; published 23 January 2009)

We report measurements of the ^{119}Sn nuclear spin-echo decay rate $1/T_{2G}$ in the heavy-fermion compound USn_3. From $1/T_{2G}$, the magnetic spin-spin correlation length ξ is found to vary as $\xi \sim T^{-3/4}$ above $\sim$100 K, which is expected for a quantum critical regime at high temperatures. Combined with the spin-lattice relaxation rate $1/T_1$, T_1T/T_{2G}^2 is found to be temperature independent in the heavy-fermion state below $T^* \sim 30$ K. This indicates that the heavy-fermion state of USn_3 is categorized in the overdamped regime with a dynamical critical exponent $z = 2$. These observations are consistent with a spin density wave magnetic instability at the quantum critical point.

DOI: 10.1103/PhysRevLett.102.037208 PACS numbers: 75.30.Mb, 76.60.−k

The heavy-fermion state is generally near a quantum critical point (QCP) of magnetic instability at 0 K because of competition between the Ruderman-Kittel Kasuya-Yosida interaction and the Kondo effect [1]. Recently, the nature of the QCP in heavy-fermion compounds has piqued considerable interest, since two different models have been proposed to describe this effect. If the magnetic instability has an itinerant antiferromagnetic spin density wave (SDW) origin [2,3], quantum critical behaviors appear next to the heavy-fermion state of the overdamped regime with dynamical critical exponent $z = 2$ and scaling dimension $\eta = 0$. In contrast, if spin localization is the origin of the instability [4,5], behaviors around the QCP belong to a different universality class with an E/T scaling law for magnetic susceptibility. The nature of the QCP has been investigated mainly in $4f$ ($4f^1$) Ce-based heavy-fermion systems up to now. The SDW type has been confirmed for $CeRu_2Si_2$ [6,7]. In contrast, a spin localization transition with localization of f electrons has been proposed for $CeCu_{5.9}Au_{0.1}$ [8]. The nature of the QCP depends on the character of the f electrons (more exactly of the f electron Fermi surface). In order to further examine this question, it is useful and appropriate to determine the type of QCP found in $5f$ U-based heavy-fermion compounds, which have a different (i.e., more itinerant, $5f^2$) f-electron character.

In heavy-fermion f-electron compounds, magnetic f moments have a localized character coupled through the Ruderman-Kittel Kasuya-Yosida interaction at high temperatures. Below a certain characteristic temperature T^*, the f-electron moments are screened dynamically with conduction electrons by the Kondo effect, and finally, a strongly renormalized Fermi-liquid state with a large effective mass, i.e., the heavy-fermion state, appears.

In order to investigate the QCP of U-based heavy-fermion compounds quantitatively based on a certain theoretical model, USn_3 is an ideal compound, since USn_3 has a simple cubic structure with U sites having cubic local symmetry (Fig. 1) and a large Sommerfeld specific heat constant $\gamma = 170$ mJ/mol K^2 with a paramagnetic ground state [9,10]. In addition, a high-quality sample with a very low impurity level (e.g., residual resistivity $\sim$1.7 $\mu\Omega$ cm) can be obtained. Figure 1 shows the T dependence of the static magnetic susceptibility χ of USn_3. At high temperatures, Curie-Weiss behavior with a reduced effective moment $\mu_{\rm eff} = 2.44\mu_B$ is observed, as is characteristic of itinerant systems. Below $T^* \sim 30$ K in the heavy-fermion state, χ becomes constant at $\sim 9 \times 10^{-3}$ emu/mol. The Wilson ratio $R_w \equiv (\chi/\gamma)(\pi^2 k_B^2/3\mu_B^2)$ is found to be $\sim$2, indicating that this compound is in the strongly correlated regime. The ground state of USn_3 is near to a QCP, since antiferromagnetic ordering is considered to appear with negative pressure [11].

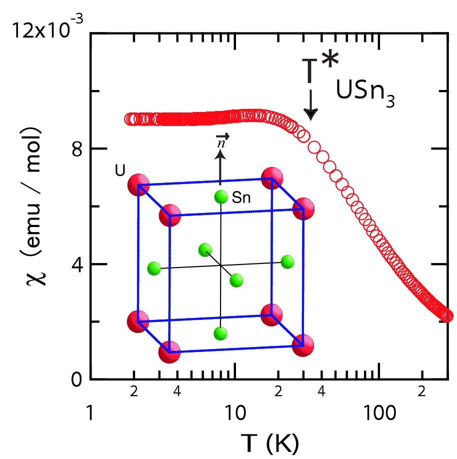

FIG. 1 (color online). T dependence of the static magnetic susceptibility χ in USn_3. Below $T^* \sim 30$ K, χ becomes constant. At high temperatures, χ obeys the Curie-Weiss law with effective moment $\mu_{\rm eff} = 2.44\mu_B$. The inset shows the cubic (face-centered cubic) crystal structure of USn_3. $\vec{n}$ indicates the local symmetry axis of the Sn site.

In our previous ^{119}Sn NMR study [12] of USn_3, the nuclear hyperfine coupling constants, the T dependence of the Knight shift and of the spin-lattice relaxation time T_1 were reported. An enhancement of antiferromagnetic fluctuations was clearly observed in the spin-lattice relaxation, which is consistent with inelastic neutron scattering measurements [13]. In this report, the quantum critical behavior in $5f$-heavy-fermion USn_3 is concluded to be consistent with the SDW description, using the spin-echo decay (T_{2G}) method, which was quite successful in elucidating the magnetic correlations of high T_c cuprates [14,15].

The spin-lattice relaxation rate $1/T_1$ probes the imaginary part of the general susceptibility $\mathrm{Im}\chi(q, \omega_n)$ at low energy $\omega_n \sim 0$ (more exactly, ω_n is the NMR measurement frequency 119 MHz $\sim$ 6 mK in this study) [16]. For $d = 3$ systems,

$$\frac{1}{T_1 T} \sim \int \frac{\mathrm{Im}\chi(q, \omega_n)}{\omega_n} d^3 q. \tag{1}$$

In contrast, the Gaussian component of the spin-echo decay rate $1/T_{2G}$ probes the real part of the general susceptibility $\mathrm{Re}\chi(q, \omega = 0)$ when indirect couplings between nuclear spins are appreciable [17,18],

$$\left(\frac{1}{T_{2G}}\right)^2 \sim \int \mathrm{Re}\chi(q, 0)^2 d^3 q. \tag{2}$$

Based on the dynamical scaling law, $\chi(q, \omega) = \xi^{2-\eta} g(\xi q, \xi^z \omega)$ with a scaling function g for the SDW case [19], one can obtain dynamical scaling relations [14,15],

$$\frac{1}{T_1 T} \sim \xi^{z-1-\eta}, \qquad \left(\frac{1}{T_{2G}}\right)^2 \sim \xi^{1-2\eta}. \tag{3}$$

In the overdamped regime ($z = 2$, $\eta = 0$) [2,3], $1/T_1 T \sim \xi$ and $1/T_{2G}^2 \sim \xi$, we find that $T_1 T/T_{2G}^2 \sim$ const [20]. In contrast, $T_1 \sim$ const, $T_{2G} \sim$ const, and $T_1 T/T_{2G}^2 \sim T$ are expected for the localized moment regime. It should be noted that no universal law for $T_1 T/T_{2G}^2$ around the magnetic instability can be obtained for the spin localization case, since there is no universal behavior for the magnetic correlation length ξ.

The conventional two-pulse spin-echo method is applied to determine the spin-spin relaxation time. ^{119}Sn ($I = 1/2$) nuclear spin-echo decay was measured at 119 MHz using the usual $\pi/2$-π rf pulses with time separation τ in single-crystal and powder samples for $H \perp \vec{n}$ ($\vec{n}$ is the principal axis of the Sn site indicated in the inset of Fig. 1) [12]. The line width is less than 0.15 MHz; thus, the whole ^{119}Sn NMR line was excited by the rf pulses. The ^{119}Sn nuclear spin-echo decay rates were determined by fitting the τ dependence of spin-echo intensity $M(2\tau)$,

$$M(2\tau) = M(0) \exp\left(-\frac{2\tau}{T_{2L}}\right) \exp\left(-\frac{(2\tau)^2}{2T_{2G}^2}\right), \tag{4}$$

where the first and second exponential factors are the Lorentzian and Gaussian components, respectively. As shown in Fig. 2(a), the experimental spin-echo decay curves are well reproduced by a fitting based on Eq. (4). Figure 2(b) shows the $(2\tau)^2$ dependence of the Gaussian component after dividing out the Lorentzian component. The good linearity indicates that the whole NMR line is excited uniformly, which guarantees that T_{2G} is correctly determined.

The Lorentzian rate $1/T_{2L}$ (for $H \perp \vec{n}$) is the contribution from the spin-lattice relaxation process, which is found to be $\sim 0.7/T_{1H\perp\vec{n}}$ for the whole temperature range. This value is consistent with the expected value [21] $1/T_{2L} = (1/T_{1H\perp\vec{n}} + 1/T_{1H\parallel\vec{n}})/2 \sim 0.8/T_{1H\perp\vec{n}}$. It should be noted that the anisotropy of T_1, $T_{1H\parallel\vec{n}}/T_{1H\perp\vec{n}} \sim 1.6$, is independent of T in USn_3 [12].

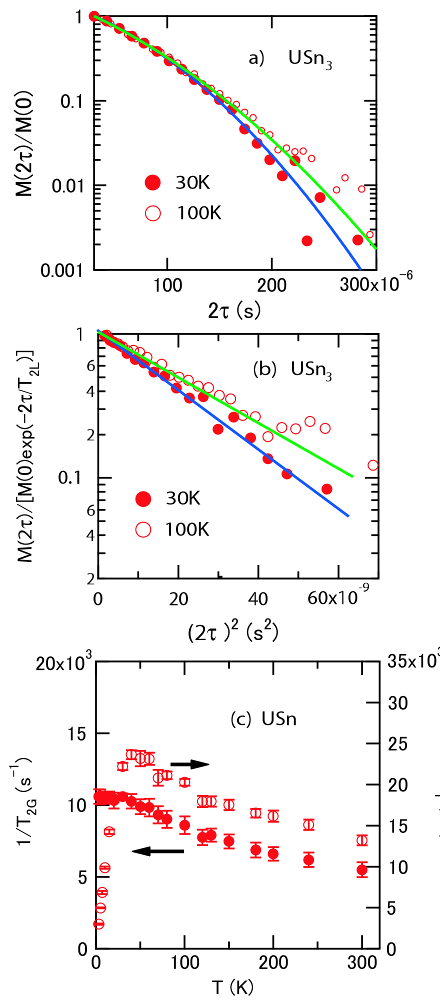

FIG. 2 (color online). (a) Spin-echo decay curves for the ^{119}Sn NMR for $H \perp \vec{n}$ in USn_3. The solid lines are fitted curves based on Eq. (4). (b) The Gaussian component of the spin-echo decay is plotted after subtraction of the Lorentzian component $\exp(-2\tau/T_{2L})$. The solid lines are fitted curves with $1/T_{2G} = 1.06 \times 10^4$ s^{-1} (30 K), 0.86×10^4 s^{-1} (100 K) and based on Eq. (4). (c) T dependence of the ^{119}Sn NMR Gaussian decay rate $1/T_{2G}$ and of the spin-lattice relaxation rate $1/T_1$ for $H \perp \vec{n}$ [12].

The Gaussian rate $1/T_{2G}$ is the contribution from nuclear spin-spin coupling. Using the second-moment method [22], the classical direct dipole-dipole coupling contribution $1/T_{2Gd-d}$ to ^{119}Sn spin-spin coupling is estimated as $1/T_{2Gd-d} \sim (2\pi)^{-1}\sqrt{\langle\Delta\omega^2\rangle} \sim 10^2$ s^{-1}, which is much smaller than the observed $1/T_{2G}$. This indicates that the nuclear spin-spin relaxation is substantially enhanced by indirect spin-spin couplings [17,18] due to antiferromagnetic ($q = Q$) fluctuations of quasiparticles, as well as by the nuclear spin-lattice relaxation [23].

The isotopic dependence of T_{2G} for ^{117}Sn ($I = 1/2$) and ^{119}Sn was determined at 150 K to be $^{117}T_{2G}/^{119}T_{2G} \sim 1.18$, which agrees well with the predicted isotopic dependence of T_{2G}: $(\gamma_{119}^2\sqrt{P_{119}})/(\gamma_{117}^2\sqrt{P_{117}}) = 1.16$, where γ and P are the nuclear gyromagnetic ratio and the isotopic abundance of ^{117,119}Sn, respectively [24].

Figure 2(c) shows the T dependence of $1/T_1$ and $1/T_{2G}$ for $H \perp \vec{n}$. Below T^*, $1/T_1$ becomes proportional to T (Korringa behavior) due to the formation of the heavy-fermion state. At high temperatures, $1/T_1$ starts to saturate as expected for a localized-like case, although actual itinerant character still persists [12]. The behavior below T^* is different; i.e., $1/T_{2G}$ becomes nearly constant. The T dependence of T_1T/T_{2G}^2 is presented in Fig. 3(a). Below $\sim T^*$ in the heavy-fermion state, T_1T/T_{2G}^2 is constant as expected for the overdamped case. In the framework of the SDW model ($z = 2$, $\eta = 0$) developed by Moriya [3], the constant value of T_1T/T_{2G}^2 in the overdamped regime corresponds approximately [15] to $\pi P_{119}\gamma_{119}^2A^2T_0/(8T_A)$ for a case of $I = 1/2$ NMR. Here, $A \sim \sqrt{0.5(86^2 + 59^2)} \cong 74$ kOe$/\mu_B$, $T_0 \sim 33$ K $\sim T^*$, and $T_A \sim 44$ K are the previously determined hyperfine coupling constant and two characteristic spin fluctuation temperatures for USn_3, respectively [12]. These parameters give $\pi P_{119}\gamma_{119}^2A^2T_0/(8T_A) \sim 1.0\times10^5$ K s^{-1}, in satisfactory agreement with the observed constant $T_1T/T_{2G}^2 \sim 1.1\times10^5$ K s^{-1} below T^*.

As T increases above T^*, T_1T/T_{2G}^2 begins to increase, indicating that the dynamical scaling relation has broken down. From Eqs. (1) and (2), $1/TT_1$ and $1/T_{2G}^2$ are proportional to $\mathrm{Im}\chi(q, \omega \sim 0)$ and $\mathrm{Re}\chi(q, 0)^2$, respectively. In addition, from the Kramers-Kronig relation, $\mathrm{Re}\chi(q, 0)$ may be derived from ω integration of $\mathrm{Im}\chi(q, \omega)$ up to $\omega = \infty$:

$$\mathrm{Re}\,\chi(q, 0) = \int_0^\infty \frac{\mathrm{Im}\chi(q, \omega)}{\omega}d\omega. \tag{5}$$

Considering these relations, the present T dependence of T_1T/T_{2G}^2 implies that enhancement of $\mathrm{Im}\chi(q, \omega)$ appears near $\omega \sim 0$ as T decreases toward T^*, which is consistent with the formation of a narrow Kondo-coherence peak at the Fermi level. At high temperatures, $T_1T/T_{2G}^2 \sim T^\phi$ shows an exponent $\phi \sim 0.7$, which is smaller than the expected value $\phi = 1$ for localized systems, perhaps due to residual itinerant character. These behaviors are considered to be characteristic of $\mathrm{Im}\chi(q, \omega \sim 0)$ in the crossover regime to the heavy-fermion state [25].

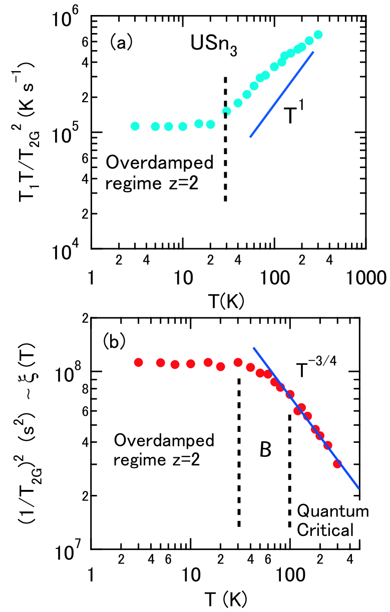

FIG. 3 (color online). (a) The T dependence of T_1T/T_{2G}^2. Below $T^* \sim 30$ K, T_1T/T_{2G}^2 becomes constant. This means that dynamical scaling behavior appears in the heavy-fermion state. Above T^*, the experimental T dependence of T_1T/T_{2G}^2 can be expressed as $T_1T/T_{2G}^2 \sim T^\phi$ ($\phi \sim 0.7$). (b) T dependence of $1/T_{2G}^2 \sim \xi(T)$. $\xi(0)$ is estimated as $\xi(0)/a \sim 3.4$ where a is the lattice constant (see text). Crossover boundaries between overdamped, intermediate B and quantum critical regimes are indicated by broken lines.

The dynamical scaling relation between $1/T_1T$ and the magnetic correlation length ξ in Eq. (3) is no longer valid above T^*. Nevertheless, the T dependence of ξ can be estimated from $1/T_{2G}$. Although the dynamical scaling relation breaks down around $\omega \sim 0$ due to the enhancement of $\mathrm{Im}\chi(q, \omega \sim 0)$, the static scaling law $\mathrm{Re}\chi(q, 0) \sim \xi^2 g(q\xi, 0)$ still holds approximately at high temperatures [26]. This leads to $1/T_{2G}^2 \sim \xi(T)$ in Eq. (3). As shown in Fig. 3(b), $\xi(T) \sim T^{-3/4}$ at temperatures above $\sim$100 K. This behavior is in fact expected for the SDW quantum critical regime in ($d = 3$, $z = 2$) heavy-fermion systems [27,28], but does not agree with the usual scaling behavior $\xi(T) \sim T^{-1/z} \sim T^{-1/2}$. In the overdamped heavy-fermion regime below 30 K, ξ becomes nearly saturated. This can be interpreted as the expected behavior of a Fermi liquid: $[\xi(T)/\xi(0)]^2 \sim (1 - bT^2)$, with a small constant $b \ll 1$. The absolute value of $\xi(0)$ can be estimated from the SDW model [3], $\xi(0)/a \sim 1.6/\sqrt{y_0} \cong 3.4$, where $a = 4.626$ Å is the lattice constant, and $y_0 \equiv 1/[2T_A\chi(Q, 0)_{T=0\ \mathrm{K}}] \sim 0.22$, from the previous result [12]. Between the overdamped regime and the quantum critical regime, there is an intermediate regime indicated as B in Fig. 3(b), where ξ is determined by the control parameters r and T in a complex way. This experimentally determined phase diagram agrees with one that was theoretically proposed [27] for the vicinity of the SDW quantum critical point in Fermi liquid systems as presented in Fig. 4. In USn_3, as well as

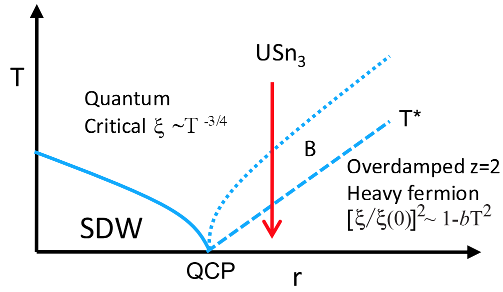

FIG. 4 (color online). Phase diagram around the SDW QCP in a Fermi liquid system [27]. r represents the control parameter for magnetic instability. The present study of USn_3 gives a clear experimental example, which shows crossovers between three different regimes.

$CeRu_2Si_2$, quantum critical behavior can be interpreted in terms of a SDW scenario.

In conclusion, the T dependence of the ^{119}Sn nuclear spin-echo decay rate $1/T_{2G}$ has been determined in the heavy-fermion compound USn_3. In the heavy-fermion state below $T^* \sim 30$ K, dynamical scaling behavior ($T_1T/T_{2G}^2 \sim$ const) for the overdamped regime ($d = 3$, $z = 2$, and $\eta = 0$) has been observed. The T dependence of the magnetic correlation length ξ determined from data for $1/T_{2G}$ shows quantum critical behavior $\xi \sim T^{-3/4}$ above $T \sim 100$ K after showing intermediate behavior between $\sim$30 K and $\sim$100 K. Such behavior is expected for a QCP in a Fermi liquid system with a SDW instability.

Considering the stable itinerant nature of the $5f$ Fermi surface in a U-based heavy-fermion system, the SDW state may be more favorable for QCP behavior than the spin-localized state with shrinkage of the Fermi surface. In order to realize spin-localized instability, e.g., of $CeCu_{5.9}Au_{0.1}$, localized $\leftrightarrow$ itinerant (small $\leftrightarrow$ large) Fermi surface instability and magnetic instability should occur at the same time. This may be expected for systems very near the Kondo regime with a small Kondo temperature and possessing a particular two-dimensional Fermi surface topology without nesting instability [5].

We thank Y. Itoh, S. Raymond, H. Yasuoka, G. H. Lander, and J. Flouquet for stimulating discussions. This work was supported by a Grant-in-Aid for Scientific Research on Innovative Areas "Heavy Electrons" (No. 20102006) of The Ministry of Education, Culture, Sports, Science, and Technology, Japan.

[1] J. Flouquet, in *Progress in Low Temperature Physics*, edited by W. Halperin (Elsevier, Amsterdam, 2005), Vol. XV, p. 3.
[2] A. J. Millis, Phys. Rev. B **48**, 7183 (1993).
[3] T. Moriya and T. Takimoto, J. Phys. Soc. Jpn. **64**, 960 (1995).
[4] P. Coleman, Physica B (Amsterdam) **259**, 353 (1999).
[5] Q. Si, S. Rabello, K. Ingersent, and J. L. Smith, Nature (London) **413**, 804 (2001).
[6] H. Kadowaki, M. Sato, and S. Kawarazaki, Phys. Rev. Lett. **92**, 097204 (2004).
[7] H. Kadowaki, Y. Tabata, M. Sato, N. Aso, S. Raymond, and S. Kawarazaki, Phys. Rev. Lett. **96**, 016401 (2006).
[8] A. Schröder, G. Aeppll, R. Coldea, M. Adams, O. Stockert, H. v. Löhneysen, E. Bucher, R. Ramasashvill, and P. Coleman, Nature (London) **407**, 351 (2000).
[9] M. R. Norman, S. D. Bader, and H. A. Kierstead, Phys. Rev. B **33**, 8035 (1986).
[10] K. Sugiyama, T. Iizuka, D. Aoki, Y. Tokiwa, K. Miyake, N. Watanabe, K. Kindo, T. Inoue, E. Yamamoto, Y. Haga, and Y. Ōnuki, J. Phys. Soc. Jpn. **71**, 326 (2002).
[11] D. Kaczorowski, J. Phys. Soc. Jpn. **75** Supplement, 68 (2005).
[12] S. Kambe, H. Sakai, Y. Tokunaga, T. D. Matsuda, Y. Haga, H. Chudo, and R. E. Walstedt, Phys. Rev. B **77**, 134418 (2008).
[13] M. Loewenhaupt and C.-K. Loong, Phys. Rev. B **41**, 9294 (1990).
[14] N. J. Curro, T. Imai, C. P. Slichter, and B. Dabrowski, Phys. Rev. B **56**, 877 (1997).
[15] Y. Itoh and T. Machi, arXiv:0804.0911v2, and references therein.
[16] T. Moriya, Prog. Theor. Phys. **16**, 641 (1956).
[17] C. H. Pennington and C. P. Slichter, Phys. Rev. Lett. **66**, 381 (1991).
[18] R. E. Walstedt and S.-W. Cheong, Phys. Rev. B **51**, 3163 (1995).
[19] For example, P. M. Chaikin and T. C. Lubensky, *Principles of Condensed Matter Physics* (Cambridge University Press, Cambridge, 1995).
[20] If ξ becomes T independent, T_1T/T_{2G}^2 becomes constant for any z value. However, $z = 2$ is suggested in this case since $z = 1$ and 3 cases are unlikely for a $d = 3$ antiferromagnetic heavy-fermion state [2].
[21] A. Narath, Phys. Rev. B **13**, 3724 (1976).
[22] For example, C. P. Slichter, *Principles of Magnetic Resonance* (Springer, New York, 1990), 3rd ed..
[23] The hyperfine form factor $f(q)$ at the Sn site is taken into account to estimate the enhancement of antiferromagnetic correlations from $1/T_1$ results [12]. In this Letter $f(q)$ is not described explicitly, since none of the essential discussion is affected by it.
[24] C. H. Pennington, D. J. Durand, C. P. Slichter, J. P. Rice, E. D. Bukowski, and D. M. Ginsberg, Phys. Rev. B **39**, 274 (1989).
[25] In Ref. [12], the T dependence of the effective Ruderman-Kittel Kasuya-Yosida interaction J_Q is introduced in order to interpret the crossover regime. However, such a description may be valid only for the low-energy part of $\mathrm{Im}\chi(q, \omega)$. A more realistic model is necessary to reproduce the whole ω dependence of $\mathrm{Im}\chi(q, \omega)$ up to high energies.
[26] For example, static scaling is established for the usual Lorentzian form $\chi(q, 0) = \xi^2/(1 + q^2\xi^2)$ with $g(x, 0) = 1/(1 + x^2)$. From Eq. (5), $\mathrm{Re}\chi(q, 0)$ is rather insensitive to modifications of $\mathrm{Im}\chi(q, \omega)$ in the vicinity of $\omega \sim 0$.
[27] S. Sachdev, *Quantum Phase Transitions* (Cambridge University Press, Cambridge, 1999).
[28] A. Ishigaki and T. Moriya, J. Phys. Soc. Jpn. **67**, 3924 (1998). In this reference, we find $\xi(T) \sim \chi_Q^{1/2} \sim T^{-3/4}$.